Friedrich-Alexander-Universität
Erlangen-Nürnberg

Advanced Laboratory Course

Electron Paramagnetic Resonance [EN]

Authors:

Saurabh Gangwar saurabh.gangwar@fau.de
Alexander Kulyabin alexander.kulyabin@fau.de

Group ♣

2023 – Summer Semester

Contents

1 Preparation

1.1 Abstract

In this experiment we measure Land'e factor of the CuSO4.

To do this, we place the sample in a magnetic field and direct radiation at it, measuring the output signal. At some frequency, resonant absorption will be observed, this is called Electron Paramagnetic Resonance. The main idea of the measurement is that we have an equation that relates this frequency, the value of the magnetic field and the Land'e factor. Thus, we can determine the Land'e factor.

Below we briefly describe the corresponding theory and our experiment, mostly following [1] and [2].

1.2 Theoretical basics

1.2.1 Absorption and emission

Consider an atom, which absorbs a photon with frequency ν. Suppose it's state had an energy E_1. Due to the conservation of energy, we have for the energy E_2 which corresponds to the state after the absorption:

$$E_2 = E_1 - h\nu \tag{1}$$

By analogy, the emission of this photon from the atom in the state with energy E_2 leads to state with energy E_1. It happens spontaneously over time constant, which is called the life time of the state. In the lattice emission of photons can be replaced by phonons - lattice vibration modes.

In the induced emission atom absorbs photon and goes to E_2 state, after goes to E_1 state, emits photon with the same frequency and in the same direction.

1.2.2 Quantum momentum and spin

Electron as quantum particle has the angular momemtum $\mathbf{l} = [\mathbf{r}, \mathbf{p}]$ which corresponds to the movement in 3D space. Eigenvalues of it's square:

$$\hat{\mathbf{l}}^2 = \hbar l(l+1)\,,\ l = 0, 1, 2, 3... \tag{2}$$

One of it's components, say, z-component, can be measured independently. It's eigenvalues:

$$l_z = \hbar m\,,\ m = -l, ... - 2, -1, 0, 1, 2, ...l \tag{3}$$

Electron has spin $\frac{1}{2}$. Eigenvalues of it's square:

$$\hat{\mathbf{s}}^2 = \hbar s(s+1)\,,\ s = \frac{1}{2} \tag{4}$$

Eigenvalues of the z-component:

$$s_z = \hbar m\,,\ m = \pm\frac{1}{2} \tag{5}$$

By analogy we get eigenvalues for the photon, replacing $\frac{1}{2}$ with 1.

For total angular momentum $\mathbf{j} = \mathbf{s} + \mathbf{l}$:

$$\hat{\mathbf{j}}^2 = \hbar j(j+1)\,,\; j = l+s, l+s-1, ...|l-s| \tag{6}$$

Eigenvalues of the z-component:

$$j_z = \hbar m\,,\; m = -l, -l+1, ...l \tag{7}$$

1.2.3 Land'e factor

Angular momentum and spin of the electron generates corresponding magnetic momentums:

$$\mu_l = -g_l \frac{\mu_B}{\hbar}\mathbf{l}\,,\; \mu_s = -g_s \frac{2\mu_B}{\hbar}\mathbf{s} \tag{8}$$

Here $\mu_B = \frac{e\hbar}{2m_e}$ is so-called Bohr's magnetron, $g_l = 1$, $g_s = 2$. This can be derived from taking non-relativistic limit in Dirac equation. The experimental result is $g_s \approx 2.0023$.

For total angular momentum, in general:

$$\mu_j = -g\frac{\mu_B}{\hbar}\mathbf{j} = -\gamma\mathbf{j}, \tag{9}$$

wheare g is called Land'e factor and γ is gyromagnetic ratio. In general, g could also be a matrix, as will be discussed later.

Lande factor for a quantum particle with known spin s, angular momentum l and total momentum j can be derived as:

$$g(s,l,j) = 1 + \frac{j(j+1) - l(l+1) + s(s+1)}{2j(j+1)} \tag{10}$$

1.2.4 Zeeman effect

The Zeeman effect consists in the splitting of atomic spectral lines under the action of a magnetic field [5]. If we consider magnetic field B along the z axis, then magnetic dipole moment of the electron lead to different values of the energy, depending on quantum number of the total momentum projection m_j, as follows from the previous section:

$$E = E_0 + g_j m_j \frac{\mu_B}{\hbar} B \tag{11}$$

Given possible values of m_j, this leads to:

$$\text{number of splits} = 2j + 1 \tag{12}$$

1.2.5 Fine and hyperfine structure

The Fine structure comes from spin-orbit interaction.

The multipole interaction between electron clouds and the nucleus causes the splitting of energy levels atoms, molecules and ions, resulting in Hyperfine structure.

The corresponding interaction terms theoretically comes from relativistic correctiones. [6]

1.2.6 Determination of Land'e factor

In this section we describe the main formula related to the experiment. We consider a sample with $j = 0$ and non-zero spin in an external magnetic field. Considering the magnetic field in z direction as $\mathbf{B} = (0, 0, B)$, for energy levels of the sample we have:

$$E = E_0 + gB\frac{\mu_B}{\hbar}s_z \tag{13}$$

For the electron (spin $s_z = \pm\frac{\hbar}{2}$) this leads to:

$$E_+ = E_- + g\mu_B B \tag{14}$$

Considering transition between the two levels by photon energy, we get:

$$h\nu = g\mu_B B \tag{15}$$

So, Land'e factor is determined by the photon frequency and the external magnetic field.

1.2.7 Larmor precession

There is an interesting fact that the frequency of the photon ν can be determine using classical model, where the electron is being considered as gyroscope with angular momentum s and corresponding anti-parallel magnetic momentum $\mu_s = \frac{g\mu_B}{\hbar}S$ placed in magnetic field B.

The torque in this model can be written in the following form:

$$D = \mu_s B \sin\alpha \tag{16}$$

The angular of the velocity precession:

$$\omega_p = \frac{D}{S\sin\alpha} \tag{17}$$

The corresponding frequency then:

$$\nu_p = g\frac{\mu_B}{h}B \tag{18}$$

1.2.8 Land'e factor with directional dependence

In general case, in non-isotropic materials, Lande factor is a matrix:

$$g = \begin{pmatrix} g_{xx} & g_{xy} & g_{xz} \\ g_{yx} & g_{yy} & g_{yz} \\ g_{zx} & g_{zy} & g_{zz} \end{pmatrix} \tag{19}$$

In particular, in the experiment we take CuSO4 crystal. This element is described by martix-valued g-factor, due to the fact that it is anisotropic in one direction, in the corresponding coordinate system it can be wtirren as:

$$g = \begin{pmatrix} g_\perp & 0 & 0 \\ 0 & g_\perp & 0 \\ 0 & 0 & g_\parallel \end{pmatrix} \tag{20}$$

Taking in account that in our experiment the element can rotate around x-direction and parameterising the rotation angle as θ, we can write for this case generalized equation for g, B and ν:

$$h\nu = \mu_B \left| \begin{pmatrix} g_\perp & 0 & 0 \\ 0 & g_\perp & 0 \\ 0 & 0 & g_\parallel \end{pmatrix} \begin{pmatrix} 0 \\ B_0 \sin\theta \\ B_0 \cos\theta \end{pmatrix} \right| \tag{21}$$

Finally, this can be represented as following dependence of the measured Lande factor on the angle:

$$g_{\text{meas}} = \sqrt{g_\parallel^2 \cos^2\theta + g_\perp^2 \sin^2\theta} \tag{22}$$

1.2.9 Paramagnetism

Paramagnetism type of magnetism that occurs in some materials when they are placed in strong magnetic field. This type materials generate their own magnetic field in the same direction. This can be described by so-called magnetic susceptibility χ, which means that if applied magnetic field strenght is H, then the material generates magnetisation $M = \chi H$, so the total magnetic field is

$$B = \mu_0(1 + \chi)H = \mu H, \tag{23}$$

where μ_0 is vacuum permeability, appearing due to the notations. [7]

1.2.10 Relaxation processes in solids

Due to the Boltzmann factor, number of particles $N(E) \sim \exp(-\beta E)$, there are more electrons on lower energy level. This means that during the passage through the substance of the radiation of the resonant frequency, absorption occurs.

After, the electrons that then went to the up level can give up their energy not only by emitting a photon, but also by interacting with the crystal lattice. [8]

Thus, resonant absorption will be observed.

1.3 Description of the experiment

1.3.1 Experimental setup

The experimental setup, containing receiver, hall probe, magnetic coils, iroc core, cavity waveguide, cavity resonator, sample holder, frequency meter, modulation-frequency generator, externally regulated power supply, frequency regulator, lock-in amplifier, signal-generator 2-channel digital oscilloscope, ESR PC, can be seen in figure 1, taken from [1].

The description:

Microwave radiation with a frequency around $9GHz$ is being generated by the Klystron , traveling through the waveguide.

A the beginning of the waveguide there is a cavity with volume which can be changed by a controller which displays the analogue frequency. Also there is voltmeter which shows the

voltage of this resonator, so, knowing the resonance of the voltage, one can determine the frequency of the radiation.

The Hall probe which tip has semiconductor elements is used to find out this dependence of the magnetic field on the control voltage by placing it into the cavity. It works on the basis of the Hall effect.

Next, the radiations goes to the center with a cavity where the experimental sample is situated. Around there is U-shaped iron core with magnetic coils which creates magnetic field in the area of the sample. The signal generator creates the voltage and the ammeter shows the current, which determines the field strength. Moreover, there are two more small coins connected with low-frequency generator, creating sinosoudal modulation signal with the frequency about 1kHz.

After going through the sample, the radiation hits a microwave receiver where the voltmeter measures it's strength. This output is sent to lock-in amplifier using $1kHz$ frequency modulation signal. After output of lock-in amplifier and the signal generator are sent to a two-channel PC oscilloscope 'Picoscope' which can display and analyze the signals.

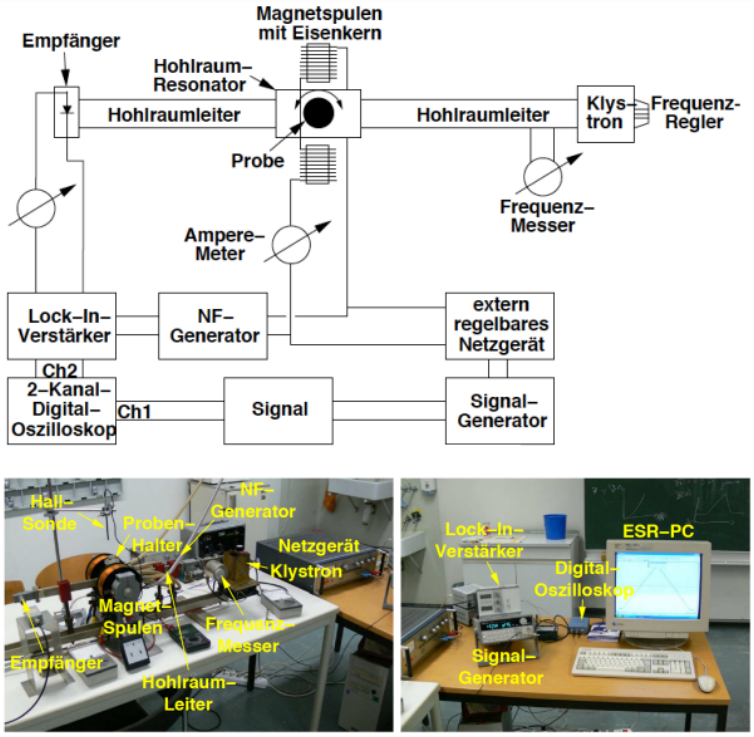

Figure 1: The scheme of the experimental setup and it's photos. Labels, translated from German: Empf¨anger (receiver), Hall-Sonde (hall probe), Magnet-Spulen (magnetic coils), Eisenkern (iroc core), Hohlraum-Leiter (cavity waveguide), Hohlraum resonantor (cavity resonator), Proben-Halter (sample holder), Frequenz-Messer (frequency meter), NF generator (modulation-frequency generator), extern regelbares Netzger¨at (externally regulated power supply), klystron and Frequency Regler (frequency regulator), Lock-in Verst¨arker (lock-in amplifier), signal-generator, the 2-Kanal Digital Oszilloscop (2-channel digital oscilloscope), and the ESR PC.

1.3.2 The plan of the experiment

At first we perform magnetic field calibration using the Hall probe. We measure the relation between the voltage on PC and the measured magnetic field for increasing and decreasing voltages.

After, we use CuSO4 as the experimental sample and perform resonance measurements, getting data set containing frequency, angle of the rotation of the sample, and magnetic field corresponding to the voltage. In each mesuremtn the voltage in automatically varied from 1.5V to 3V and back to 1.5V. We record the resonance signals using the oscilloscope 'Picoscope', which are expected to be similar to Gaussian derivative, so we are interested where they are zero in the area between max and min values.

Next, we use DPPH, for which g-factor is known and isotropic, as the experimental sample. We do the same resonance measurements to estimate the systematic error and check our previous actions.

At the end we repeat calibration of the magnetic field due to possible changes.

1.3.3 Experimental notes

Important details, based on [3]:

1. Due to the magnetic hysteresis effect the strength of the magnetic field is different depending on the sing of it's speed of changing, so we need to vary the voltage both up and down.

2. Due to the fact that the hysteresis effect and Land'e factor may depend on the range of the magnetic field, it is important to keep the corresponding voltage range the same during all the experiment.

3. According to the formula for g_{meas} we expect a periodic change of the g-factor for the $CuSO4$ and expect a it to be constant for the $DPPH$ since it is isotropic. To fully determine this dependence we theoretically need to vary the angle from 0° to 180°. In practice we are going to expand the interval for more confidence and avoiding errors.

4. We perform the magnetic field calibration using the Hall probe to find out the dependence of the magnetic field on the voltage due to the fact we don't know it for our experimental setup.

5. We perform two calibrations to find out possible changes, which may related to some processes, for example heating, during the experiment.

6. Due to the hysteresis effect dependence the magnetic behavior at first can be different, so the power supply be passed through one up-down ramp before the first calibration.

2 Magnetic field calibration

2.1 Experimental data

As described earlier, we place the Hall probe into the cavity and made measurements of the dependence of the magnetic field B on the corresponding voltage applied to the coils. We did it before the experiment and after, in both cases we varied the voltage V between $1.5\,V$ and $3\,V$, up and down.

This is important to note that there are two different voltages. First is the voltage of the actual power supply, U, which is shown on the PC screen. The other one is the voltage

generated by the function generator, V, according to which we did the calibration. However, for further analysis, we need to relate the magnetic field to the voltage displayed on the screen. This relationship can be easily established using the fact that these voltages are linearly related.

We estimate the magnetic field measurement error as 1mT due to the size of the scale and error of V as 46mV due to the modulation.

Here is the data with a linear fitting curve showing the relation between the voltages witha quadratic fitting curve for the data of the calibrations:

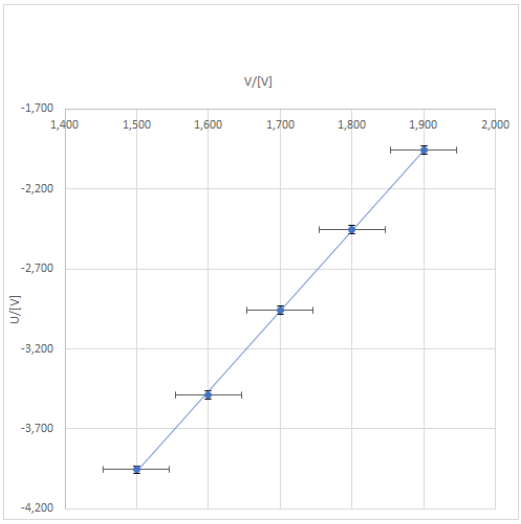

Figure 2: The dependece of U on V.This linear fitting curve with reduced Pearson's chi-squared test $\chi \approx 0.40$. Note: the error of U is assumed due to the display as 25mV, we are interested in dependence between visible values, not in the real value.

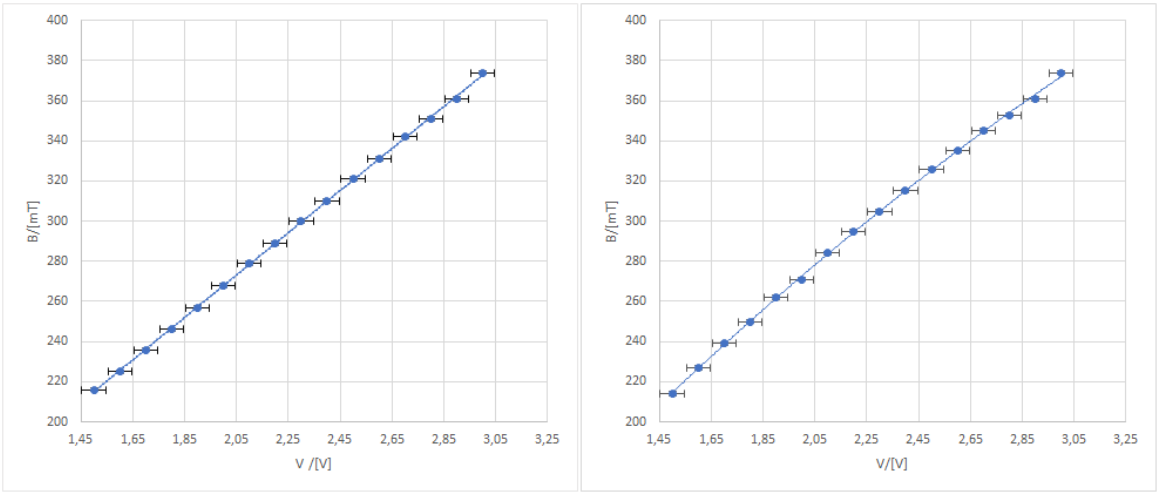

Figure 3: The dependence of the magnetic field on the voltage, respectively, with its increase (left) and decrease (right), before the experiment. This is quadratic fitting curves with reduced Pearson's chi-squared tests $\chi_{left} \approx 0.57$, $\chi_{right} \approx 3.86$.

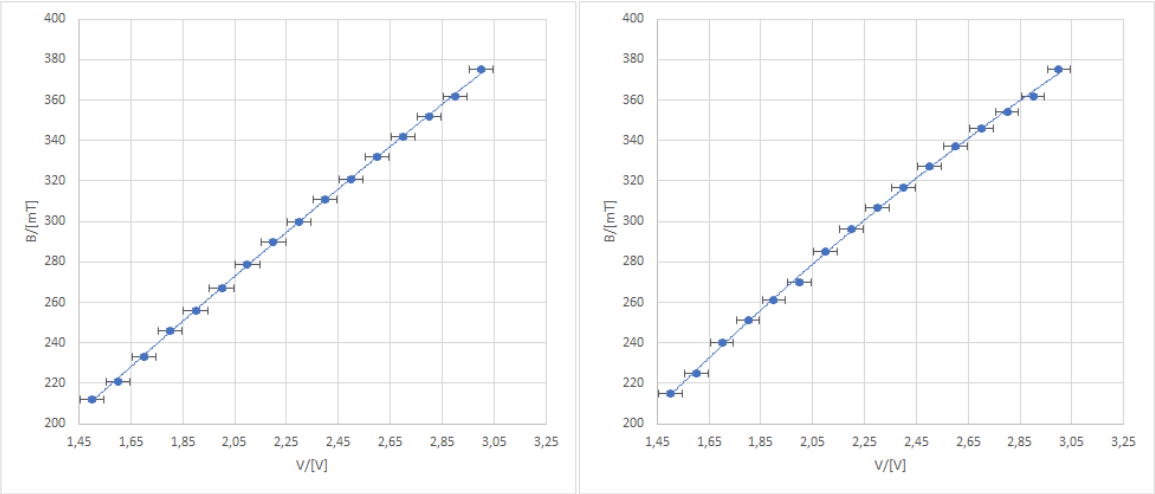

Figure 4: The dependence of the magnetic field on the voltage, respectively, with its increase (left) and decrease (right), after the experiment. This is quadratic fitting curves with reduced Pearson's chi-squared tests $\chi_{left} \approx 0.85$, $\chi_{right} \approx 2.40$.

2.2 Calibration curves

As stated before, to find the dependence of the magnetic field on the voltage, we use a quadratic fitting curve. The linear structure of the dependence is caused by considering ideal coil generating magnetic field, while it have corrections due to effects of heating, magnetic hysteresis and other. We consider the quadratic order as the simplest and sufficient.

Here are the tables which show the corresponding coefficients for the four fitting curves $B(V) = aV^2 + bV + c$, showing the change in the magnetic field at the beginning, at the end of the experiment and during it's increase or decrease and their average values.

For the case of an increase in the magnetic field:

Coeff.:	$a_{V\nearrow}$ / [mTV^{-2}]	$b_{V\nearrow}$/[mTV^{-1}]	$c_{V\nearrow}$ / [mT]
Before:	-0.63 ± 0.71	108.04 ± 0.41	54.36 ± 0.23
After:	-4.32 ± 0.59	127.68 ± 0.50	29.22 ± 0.42
Average:	-2.4 ± 0.65	117.86 ± 0.46	41.79 ± 0.34

Table 1: Fitting quadratic curve coefficients for measurements with decreasing magnetic field.

For the case of a decrease in the magnetic field:

Coeff.:	$a_{V\swarrow}$ / [mTV^{-2}]	$b_{V\swarrow}$ / [mTV^{-1}]	$c_{V\swarrow}$ / [mT]
Before:	-11.35 ± 0.28	156.05 ± 1.07	5.98 ± 0.36
After:	-12.47 ± 0.32	162.18 ± 0.84	-1.15 ± 0.17
Average:	-11.92 ± 0.30	159.12 ± 0.96	2.42 ± 0.40

Table 2: Fitting quadratic curve coefficients for measurements with increasing magnetic field.

Using the fitting line of the voltage dependence, $U = (5.03 \pm 0.04)V - (11.52 \pm 0.02)\text{V}$, it is possible to rewrite the average calibration curves fot both cases in terms of the voltage U which we can see on the computer screen.

For the up case:

$$B_{\nearrow average} = (298.71 \pm 0.35)\text{mT} + (21.17 \pm 0.06)\text{mTV}^{-1}U - (0.10 \pm 0.03)\text{mTV}^{-2}U^2 \quad (24)$$

For the down case:

$$B_{\swarrow average} = (304.32 \pm 0.42)\text{mT} + (20.78 \pm 0.13)\text{mTV}^{-1}U - (0.47 \pm 0.02)\text{mTV}^{-2}U^2 \quad (25)$$

We assume that the last two formulas determine the magnetic fields with sufficient accuracy during the measurement of the corresponding resonances.

3 DPPH sample

3.1 Experimental data

In this section we provide measurements of the resonances corresponding to the DPPH sample.

We assume known that this material is isotropic, so we don't take angle into account. However, formally we varied angle one time, doing 3 measurements without rotation and 3 measurements in perpendicular to the initial state. All is done with frequency $\nu = 8817 \pm 1$.

We considered the frequency measurement error according to its scale. We do not take into account the errors in measuring the angles, since they are small enough due to the experimental equipment. The rest of the errors are as usual.

The original output signal graphs from the PC can be found in the appendix A, here we present the resonance values of the voltage:

θ / [°]	$U_{res\nearrow}$ /[V]	$U_{res\swarrow}$ /[V]
0	1.867 ± 0.025	0.313 ± 0.025
0	1.861 ± 0.025	0.334 ± 0.025
0	1.815 ± 0.025	0.306 ± 0.025
90	1.847 ± 0.025	0.319 ± 0.025
90	2.047 ± 0.025	0.402 ± 0.025
90	1.955 ± 0.025	0.405 ± 0.025

Table 3: The values of angles and voltages of the resonances for different measurements of the DPPH sample.

3.2 Systematic error

Using the magnetic calibration equations (24)-(25) and equation (15), we calculate magnetic fields and, finally, corresponding Lande factors, for both up and down. After that, we average

the two obtained values for each measurement, since this is a common method of dealing with such experimental data.

Here are the results:

θ / [°]	$g_{\nearrow}$	$g_{\swarrow}$	g_{mean}
0	1.8644 ± 0.0036	2.0270 ± 0.0038	1.9457 ± 0.0037
0	1.8651 ± 0.0036	2.024 ± 0.0038	1.9447 ± 0.0037
0	1.8704 ± 0.0036	2.0279 ± 0.0038	1.9492 ± 0.0037
90	1.8667 ± 0.0036	2.0262 ± 0.0038	1.9464 ± 0.0037
90	1.8440 ± 0.0035	2.0152 ± 0.0037	1.9296 ± 0.0036
90	1.8543 ± 0.0035	2.0148 ± 0.0038	1.9356 ± 0.0037

Table 4: The values of angles and calculated Lande factors of the resonances for different measurements of the DPPH sample.

Comparing the received values g_{mean} with $g_{DPPH} \approx 2.0037$ (due to [1]), we evaluate the systematic error as an average deviation $g_{DPPH} - g_{mean}$. This gives:

$$\Delta_{syst} = 0.0620 \pm 0.0037 \tag{26}$$

Obtaining the values of the Lande factor for CuSO4 is completely similar and we will take into account this systematic error.

4 CuSO4 sample

4.1 Experimental data

In this part, we present the measurements for the CuSO4 sample of direct interest to us.

As described in the beginning, we rotate the experimental sample from 0° to 200° degrees which is more than sufficient. We take the step as 10°, assuming that this would be an optimal choice.

As said before, the original output signal graphs from the PC can be found in the appendix A, and here we present a table of stress resonances for different sample rotation angles. It is important to note that this time the frequency has undergone minor changes because of its regulation.

θ / [°]	ν / [MHz]	$U_{res_{\nearrow}}$ /[V]	$U_{res_{\swarrow}}$ /[V]
0	8842 ± 1	0.333 ± 0.025	-1.417 ± 0.025
10	8842 ± 1	0.311 ± 0.025	-1.425 ± 0.025
20	8836 ± 1	0.311 ± 0.025	-1.424 ± 0.025
30	8836 ± 1	0.495 ± 0.025	-1.152 ± 0.025
40	8836 ± 1	0.585 ± 0.025	-1.013 ± 0.025
50	8836 ± 1	0.860 ± 0.025	-0.830 ± 0.025
60	8837 ± 1	1.012 ± 0.025	-0.608 ± 0.025
70	8837 ± 1	1.136 ± 0.025	-0.466 ± 0.025
80	8837 ± 1	1.269 ± 0.025	-0.326 ± 0.025

θ / [°]	ν / [MHz]	$U_{res\nearrow}$ /[V]	$U_{res\swarrow}$ /[V]
90	8837 ± 1	1.270 ± 0.025	-0.307 ± 0.025
100	8837 ± 1	1.225 ± 0.025	-0.331 ± 0.025
110	8837 ± 1	1.198 ± 0.025	-0.406 ± 0.025
120	8837 ± 1	1.050 ± 0.025	-0.558 ± 0.025
130	8837 ± 1	0.863 ± 0.025	-0.737 ± 0.025
140	8837 ± 1	0.716 ± 0.025	-0.950 ± 0.025
150	8837 ± 1	0.585 ± 0.025	-1.102 ± 0.025
160	8837 ± 1	0.493 ± 0.025	-1.272 ± 0.025
170	8837 ± 1	0.403 ± 0.025	-1.340 ± 0.025
180	8837 ± 1	0.340 ± 0.025	-1.403 ± 0.025
190	8837 ± 1	0.358 ± 0.025	-1.356 ± 0.025
200	8837 ± 1	0.401 ± 0.025	-1.289 ± 0.025

Table 5: The values of angles and voltages of the resonances for different measurements of the CuSO4 sample.

4.2 Lande factor

Analogically we calculate the Lande factors for each case using (24)-(25) and equation (15).After we get mean values of g for them, what is considered as the final result for the measured Lande factor.

θ / [°]	$g_{\nearrow}$	$g_{\swarrow}$	g_{mean}
0	2.0662 ± 0.0043	2.3062 ± 0.0049	2.1862 ± 0.0046
10	2.0693 ± 0.0043	2.3077 ± 0.0049	2.1885 ± 0.0046
20	2.0693 ± 0.0043	2.3075 ± 0.0049	2.1884 ± 0.0046
30	2.0434 ± 0.0042	2.2582 ± 0.0047	2.1508 ± 0.0045
40	2.0309 ± 0.0041	2.2340 ± 0.0046	2.1324 ± 0.0044
50	1.9938 ± 0.0040	2.2301 ± 0.0045	2.0985 ± 0.0042
60	1.9740 ± 0.0039	2.1671 ± 0.0043	2.0705 ± 0.0041
70	1.9581 ± 0.0039	2.1449 ± 0.0042	2.0515 ± 0.0040
80	1.9413 ± 0.0038	2.1235 ± 0.0042	2.0324 ± 0.0040
90	1.9412 ± 0.0038	2.1207 ± 0.0042	2.0309 ± 0.0040
100	1.9468 ± 0.0038	2.1243 ± 0.0042	2.0356 ± 0.0040
110	1.9502 ± 0.0038	2.1356 ± 0.0042	2.0429 ± 0.0040
120	1.9690 ± 0.0039	2.1592 ± 0.0043	2.0641 ± 0.0041
130	1.9935 ± 0.0040	2.1878 ± 0.0044	2.0906 ± 0.0042
140	2.0131 ± 0.0041	2.2232 ± 0.0046	2.1181 ± 0.0043
150	2.0309 ± 0.0041	2.2494 ± 0.0047	2.1401 ± 0.0044
160	2.0436 ± 0.0042	2.2796 ± 0.0048	2.1616 ± 0.0045
170	2.0562 ± 0.0042	2.2920 ± 0.0048	2.1741 ± 0.0045
180	2.0652 ± 0.0043	2.3036 ± 0.0049	2.1844 ± 0.0046
190	2.0626 ± 0.0043	2.2949 ± 0.0049	2.1788 ± 0.0046

θ / [°]	$g_{\nearrow}$	$g_{\swarrow}$	g_{mean}
200	2.0565 ± 0.0042	2.2827 ± 0.0048	2.1696 ± 0.0045

Table 6: The values of angles and calculated Lande factors of the resonances for different measurements of the CuSO4 sample.

As it was shown in section 1.2.8, we expect such dependence of measured Lande factor on the angle:

$$g_{meas}(\theta + \theta_0) = \sqrt{g_{\perp}^2 \sin^2(\theta + \theta_0) + g_{\parallel}^2 \cos^2(\theta + \theta_0)} \tag{27}$$

Here we also took in account the initial angle θ_0, which is not known before the analysis.

We fit the g_{mean} , θ data by this function and get:

$$g(\theta) = \sqrt{(2.0285 \pm 0.0018)^2 \sin^2(\theta - 2.29^\circ \pm 0.56^\circ) + (2.1864 \pm 0.0017)^2 \cos^2(\theta - 2.29^\circ \pm 0.56^\circ)} \tag{28}$$

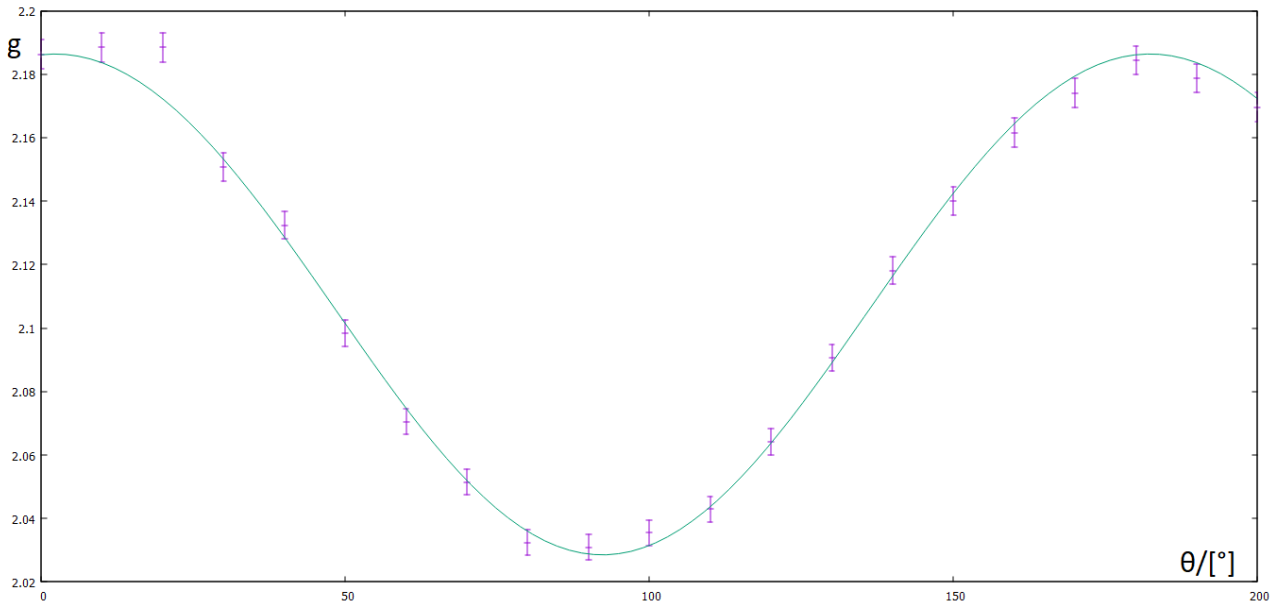

Figure 5: Dependence of the measured Lande factor on the angle.The fit curve is 28, $\chi \approx 1.23$. Note: point with $\theta = 30^\circ$ looks to be too far from the fit, however, we are sure that there are no mistake in the angle and the deviation corresponds to the order of the error, so we included this point in the analysis.

Finally, taking into account random errors and the systematic one, we get eigenvalues of the Lande factor:

$$g_{\perp} = 2.0285 \pm 0.0620 \pm 0.0041 \tag{29}$$

$$g_{\parallel} = 2.1864 \pm 0.0620 \pm 0.0041 \tag{30}$$

5 Conclusion

In this experiment, using the method of Electron Paramagnetic Resonance, we were able to get eigenvalues of the Lande factor of CuSO4.

Comparing our results with those known earlier ($g_{\parallel} \approx 2.39$, $g_{\perp} \approx 2.07$ from [4]), we can conclude that they are quite close. In particular, $g_{\perp}$ differs less than the total error. $g_{\parallel}$, however, differs more than it. It can also be seen from the plot of the measured Lande factor from the angle, that in the region of high values, there is a stronger spread.

The causes for the bigger errors, for example, may be heating and more complex type of magnetic calibration curves, just taking average values of qubic fitting curves before and after, rather than separately for each measurement, may be too simple model.

However, it seems quite difficult to increase the accuracy much using this experimental setup. According to our analysis within our method, the systematic error has the largest contribution.

A List of output signals from the PC

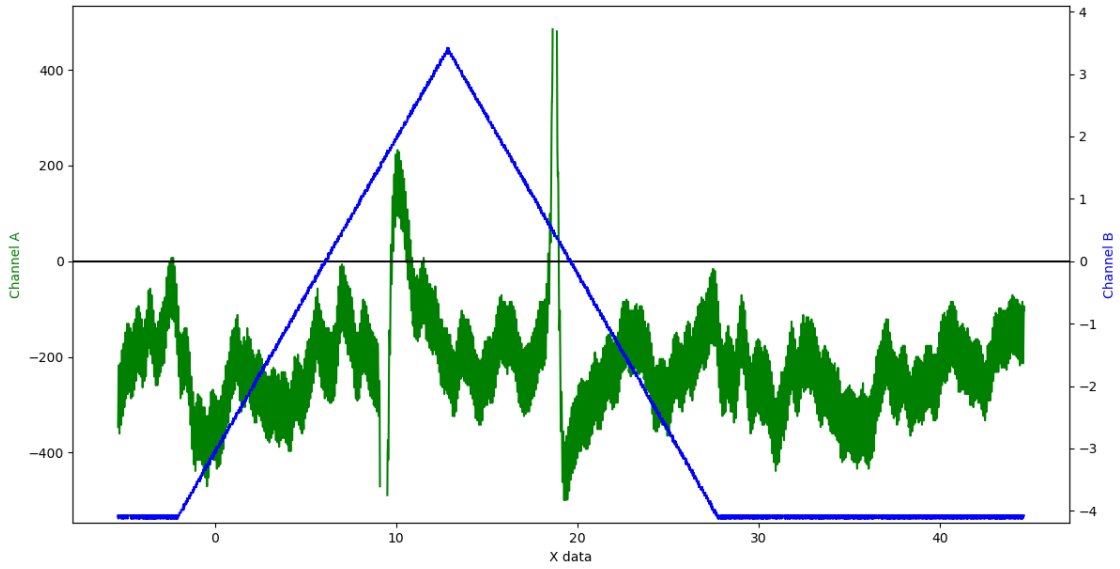

Figure 6: The output for the DPPH sample, $\theta = 0°$ (the first measurement).Chanel A is the voltage corresponding to the outgoing radiation/[mV], Chanel B is the voltage, U/[V], corresponding to the magnetic field, X data is time/[s]

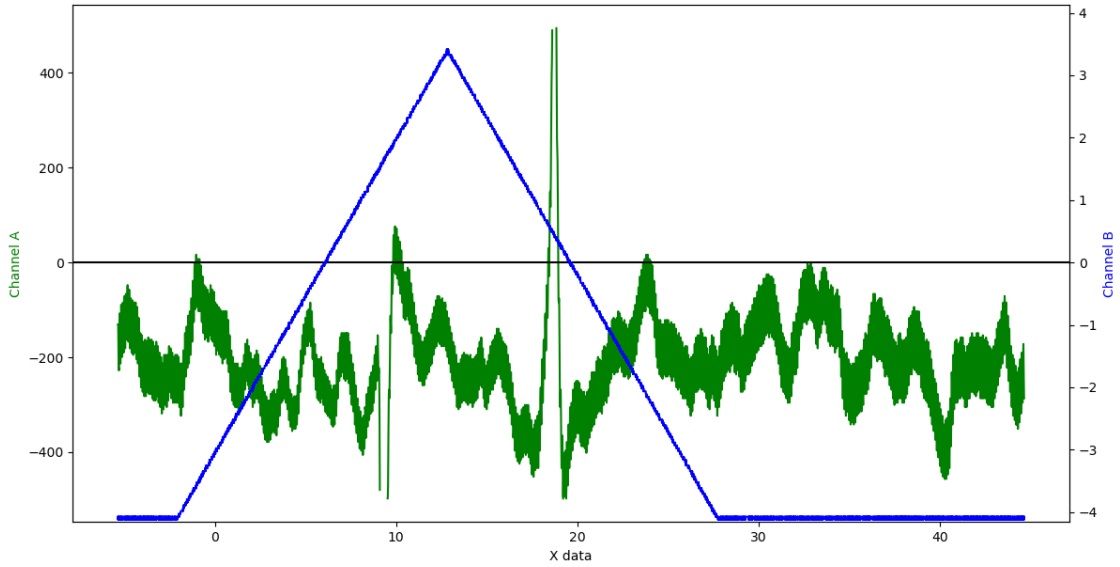

Figure 7: The output for the DPPH sample, $\theta = 0°$ (the second measurement).Chanel A is the voltage corresponding to the outgoing radiation/[mV], Chanel B is the voltage, U/[V], corresponding to the magnetic field, X data is time/[s]

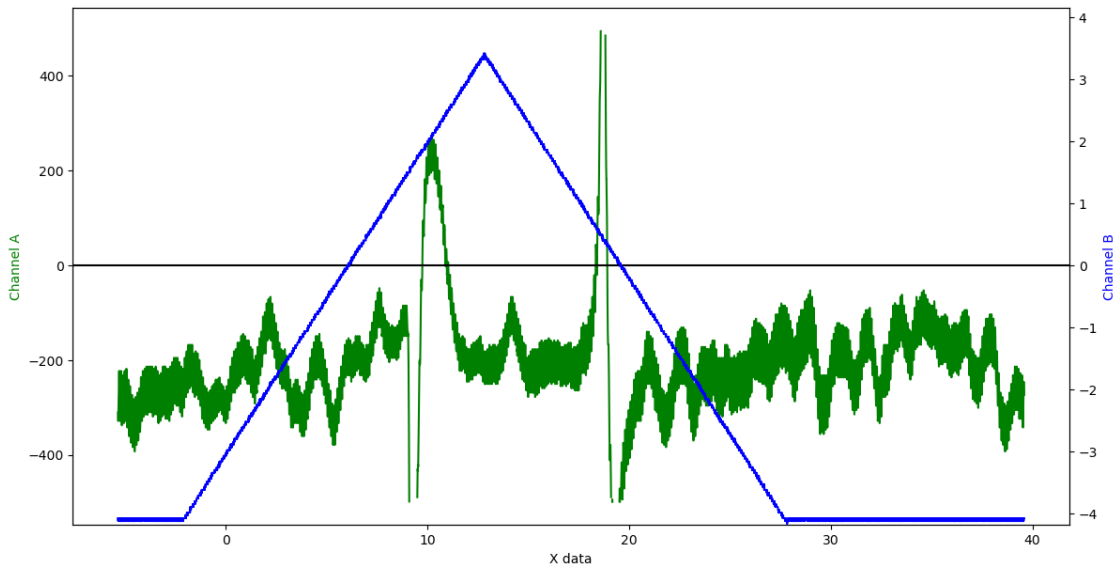

Figure 8: The output for the DPPH sample, $\theta = 0°$ (the third measurement).Chanel A is the voltage corresponding to the outgoing radiation/[mV], Chanel B is the voltage, U/[V], corresponding to the magnetic field, X data is time/[s]

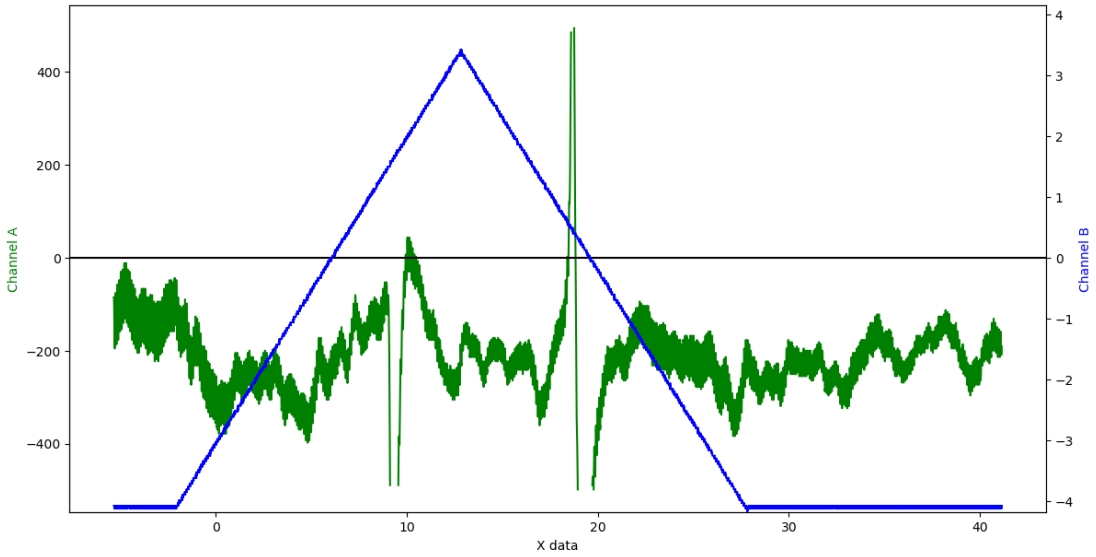

Figure 9: The output for the DPPH sample, $\theta = 90°$ (the first measurement).Chanel A is the voltage corresponding to the outgoing radiation/[mV], Chanel B is the voltage, U/[V], corresponding to the magnetic field, X data is time/[s]
Note: The first resonance looks anomalous, however, we can still find the value at the zero point and the result is also close to the rest, so we did not exclude this measurement.

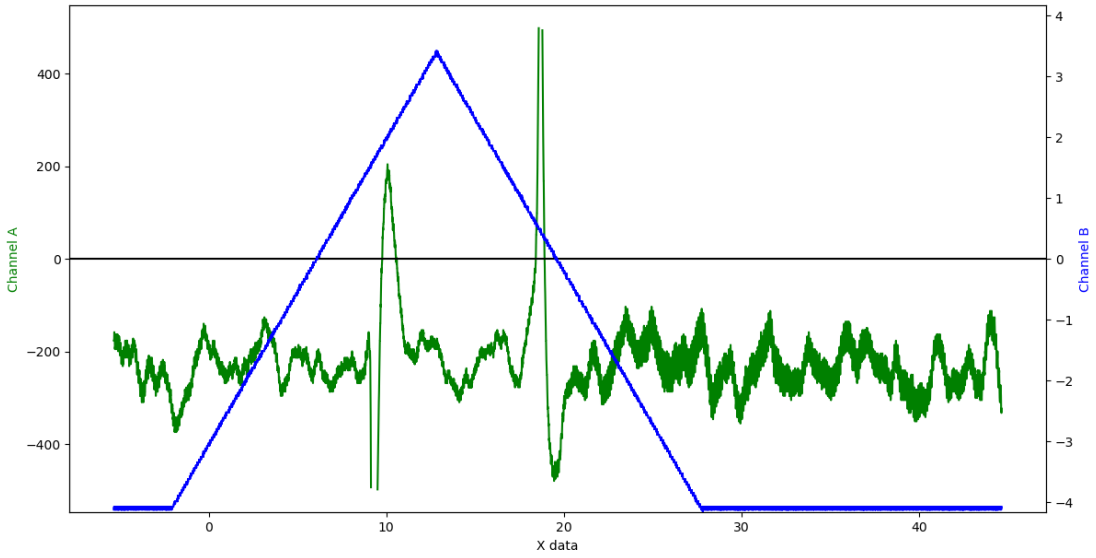

Figure 10: The output for the DPPH sample, $\theta = 90°$ (the second measurement).Chanel A is the voltage corresponding to the outgoing radiation/[mV], Chanel B is the voltage, U/[V], corresponding to the magnetic field, X data is time/[s].

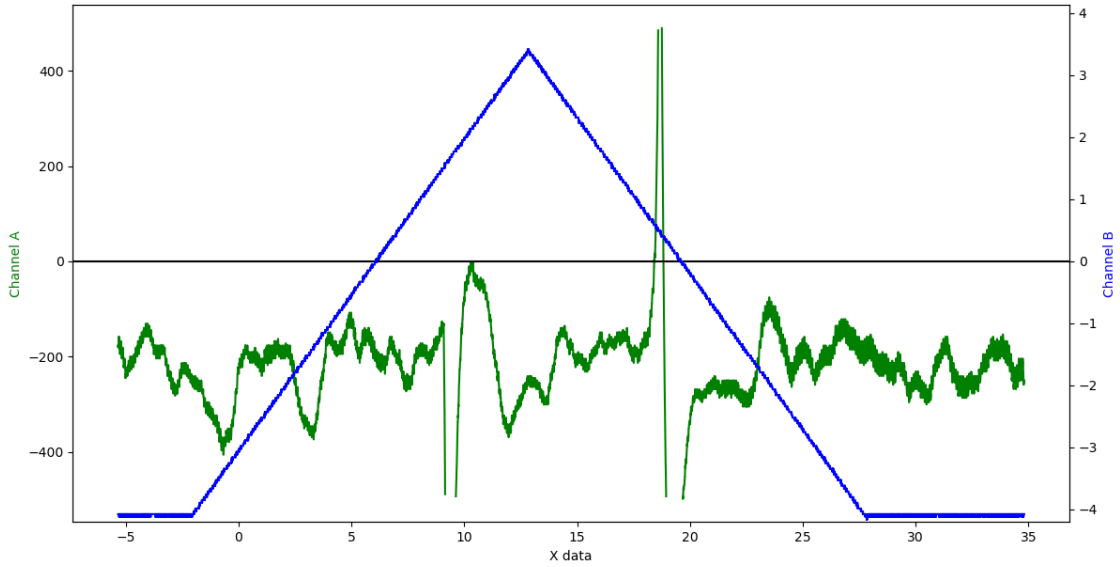

Figure 11: The output for the DPPH sample, $\theta = 90°$ (the third measurement).Chanel A is the voltage corresponding to the outgoing radiation/[mV], Chanel B is the voltage, U/[V], corresponding to the magnetic field, X data is time/[s].

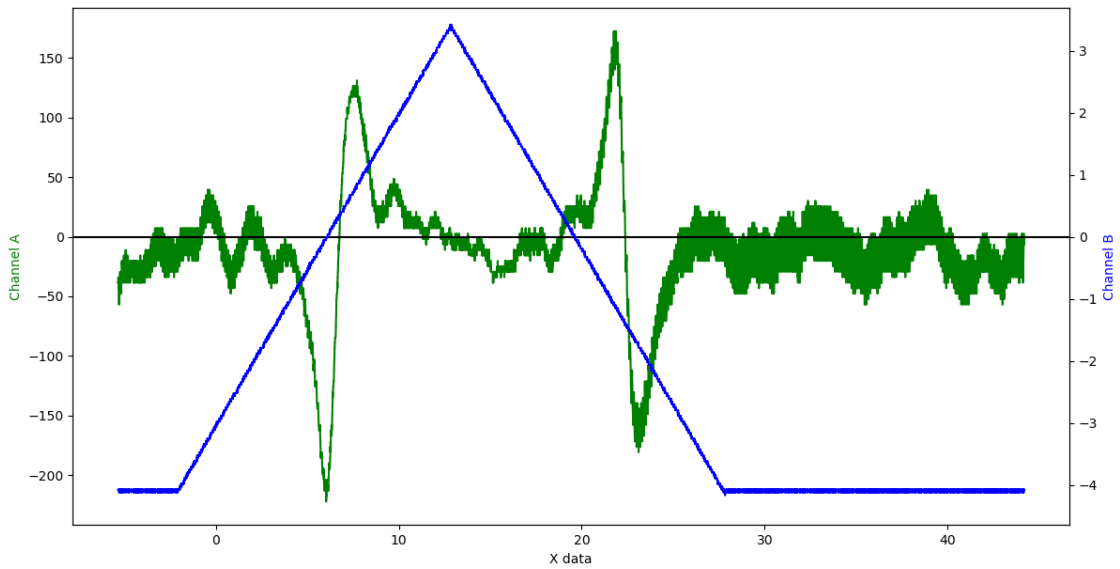

Figure 12: The output for the CuSO4 sample, $\theta = 0°$ .Chanel A is the voltage corresponding to the outgoing radiation/[mV], Chanel B is the voltage, U/[V], corresponding to the magnetic field, X data is time/[s].

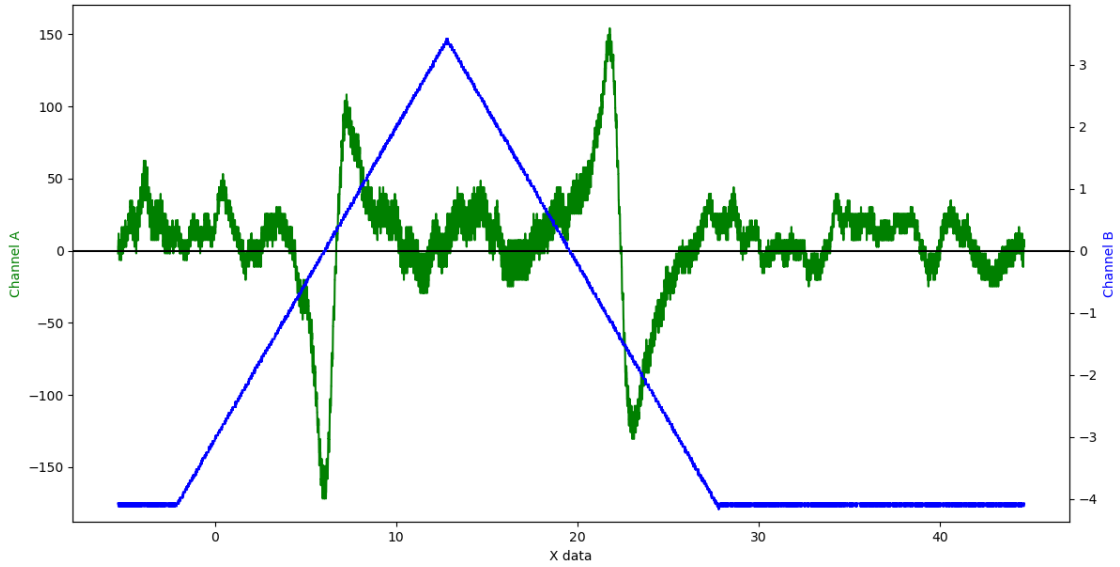

Figure 13: The output for the CuSO4 sample, $\theta = 10°$ .Chanel A is the voltage corresponding to the outgoing radiation/[mV], Chanel B is the voltage, U/[V], corresponding to the magnetic field, X data is time/[s].

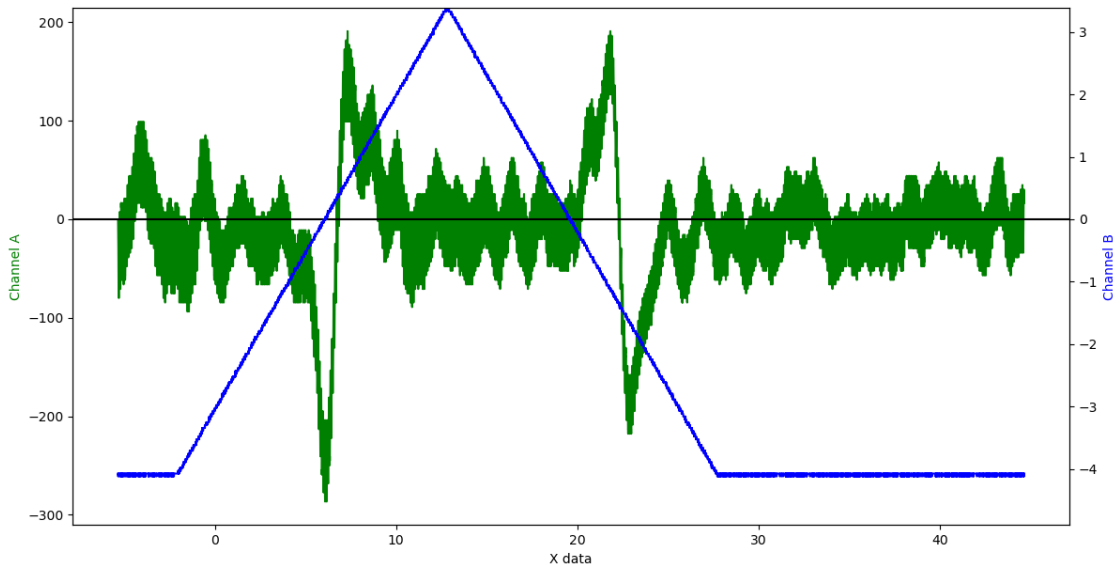

Figure 14: The output for the CuSO4 sample, $\theta = 20°$ .Chanel A is the voltage corresponding to the outgoing radiation/[mV], Chanel B is the voltage, U/[V], corresponding to the magnetic field, X data is time/[s].

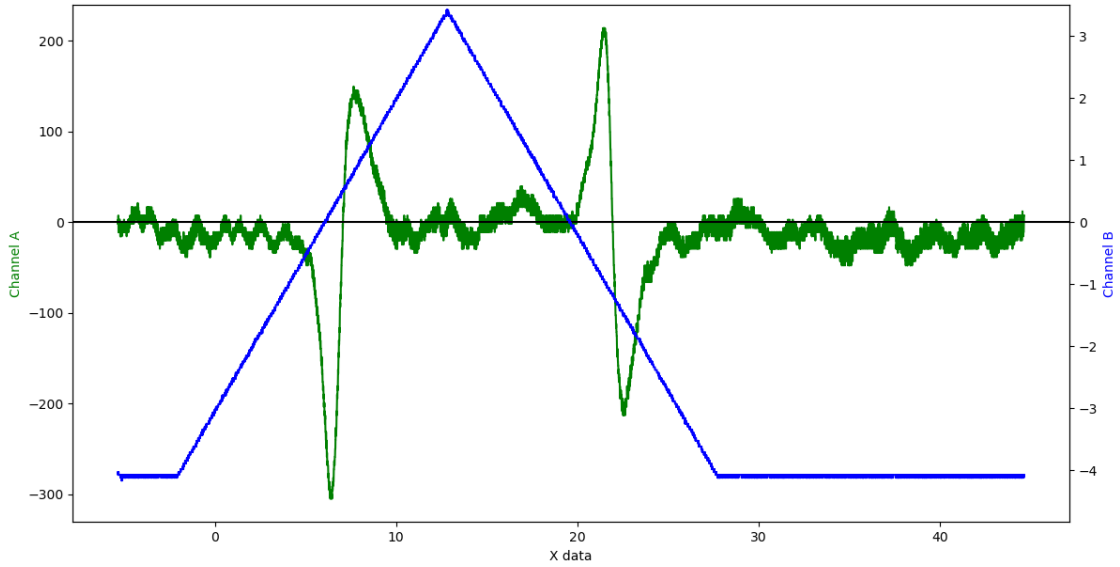

Figure 15: The output for the CuSO4 sample, $\theta = 30°$ .Chanel A is the voltage corresponding to the outgoing radiation/[mV], Chanel B is the voltage, U/[V], corresponding to the magnetic field, X data is time/[s].

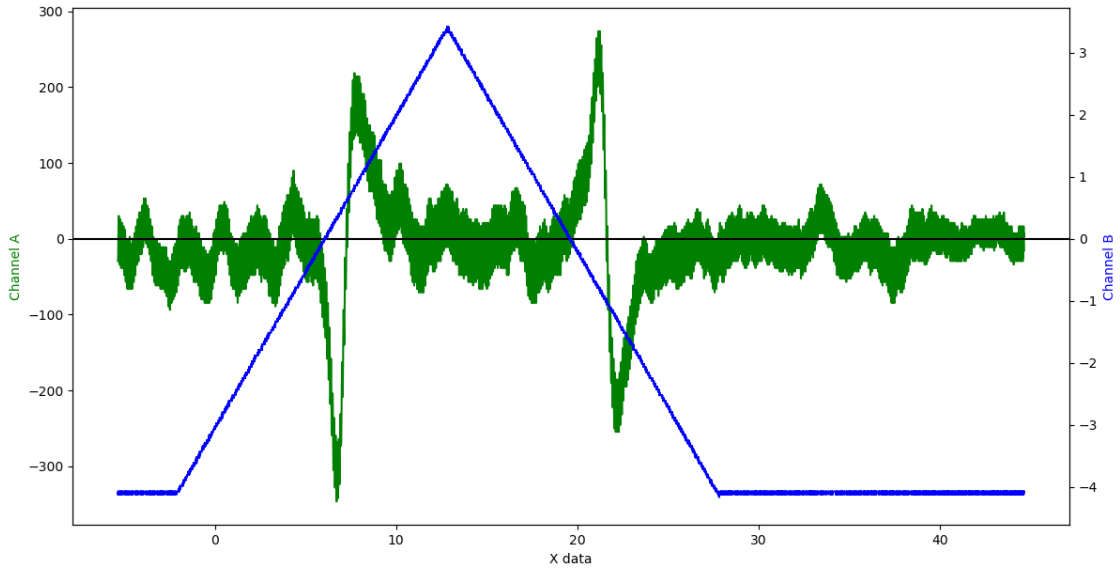

Figure 16: The output for the CuSO4 sample, $\theta = 40°$ .Chanel A is the voltage corresponding to the outgoing radiation/[mV], Chanel B is the voltage, U/[V], corresponding to the magnetic field, X data is time/[s].

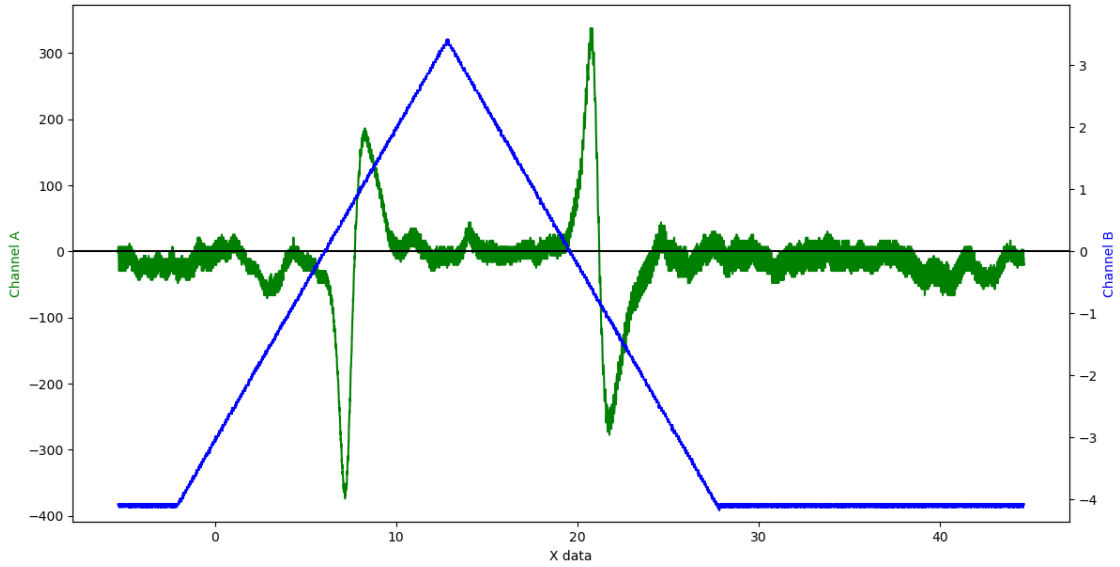

Figure 17: The output for the CuSO4 sample, $\theta = 50°$ .Chanel A is the voltage corresponding to the outgoing radiation/[mV], Chanel B is the voltage, U/[V], corresponding to the magnetic field, X data is time/[s].

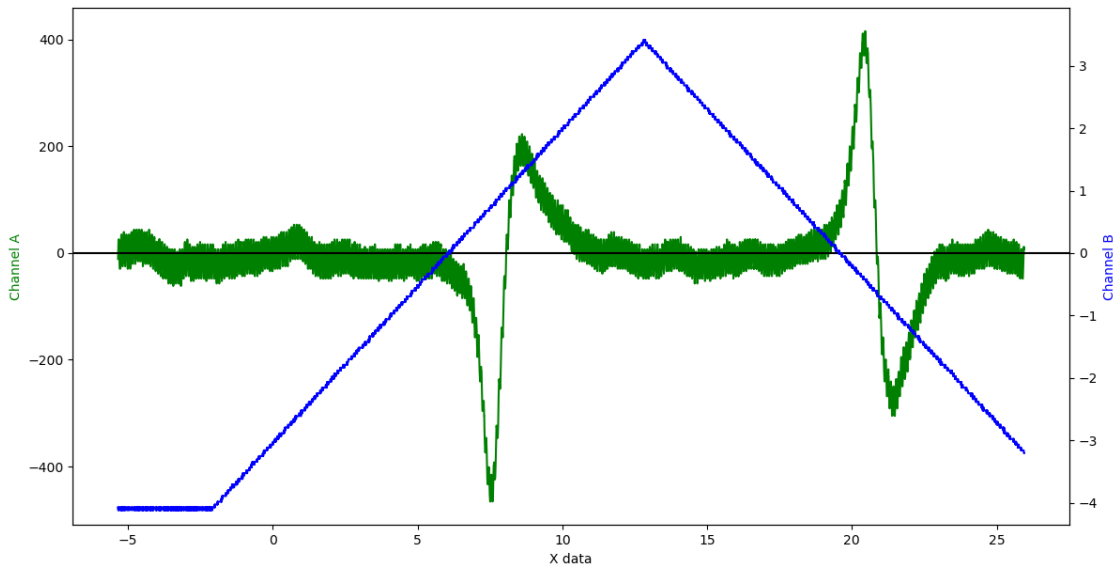

Figure 18: The output for the CuSO4 sample, $\theta = 60°$ .Chanel A is the voltage corresponding to the outgoing radiation/[mV], Chanel B is the voltage, U/[V], corresponding to the magnetic field, X data is time/[s].

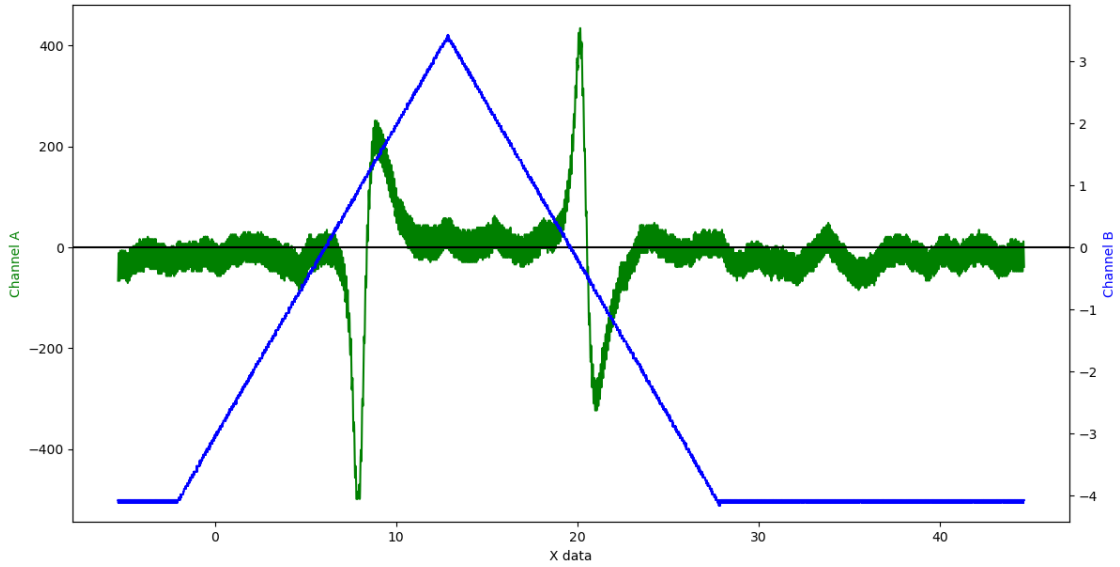

Figure 19: The output for the CuSO4 sample, $\theta = 70°$ .Chanel A is the voltage corresponding to the outgoing radiation/[mV], Chanel B is the voltage, U/[V], corresponding to the magnetic field, X data is time/[s].

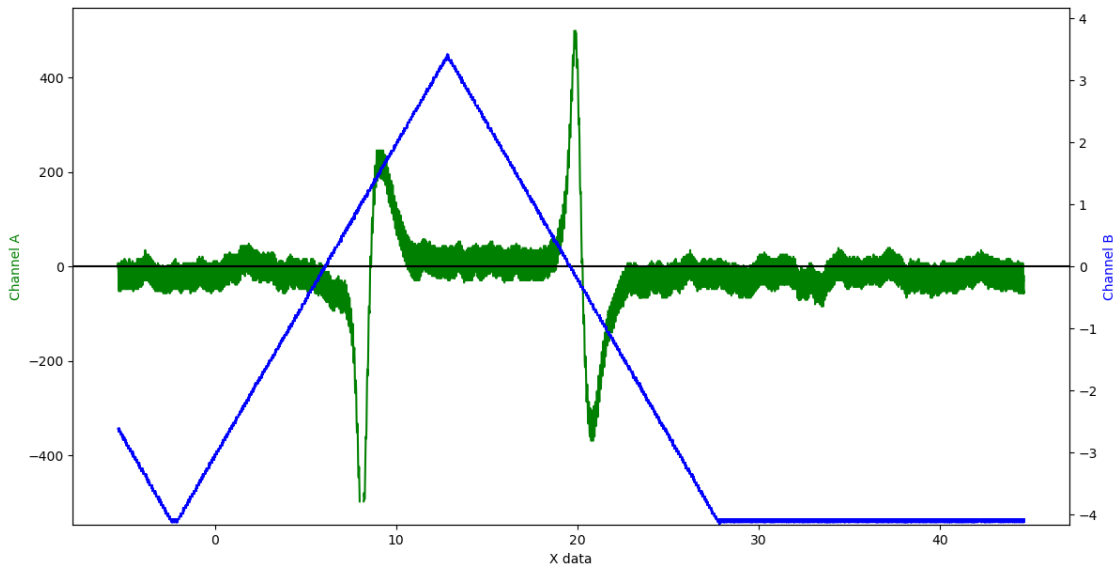

Figure 20: The output for the CuSO4 sample, $\theta = 80°$ .Chanel A is the voltage corresponding to the outgoing radiation/[mV], Chanel B is the voltage, U/[V], corresponding to the magnetic field, X data is time/[s].

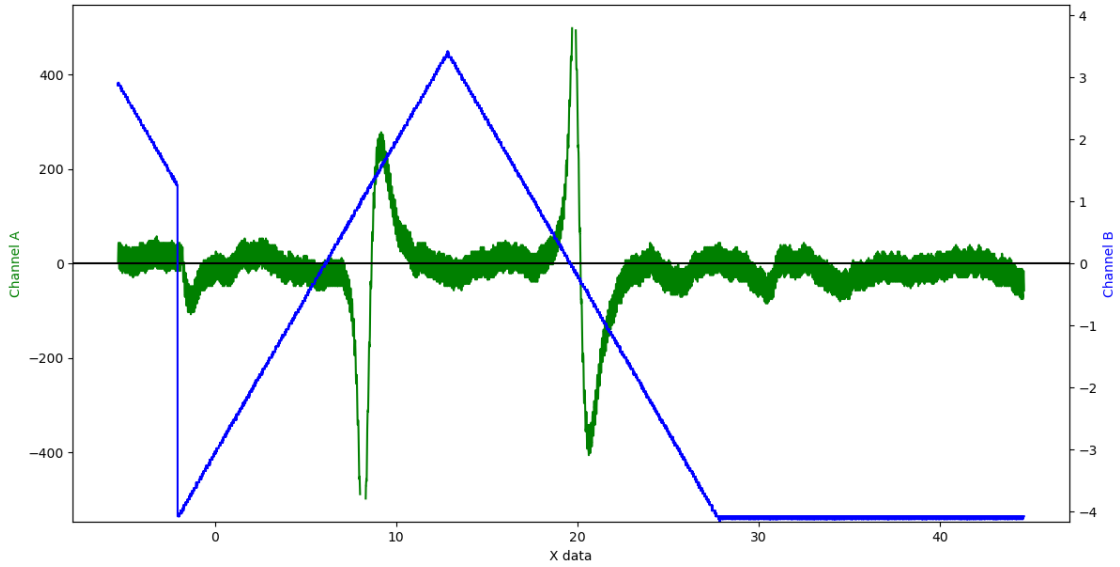

Figure 21: The output for the CuSO4 sample, $\theta = 90°$ .Chanel A is the voltage corresponding to the outgoing radiation/[mV], Chanel B is the voltage, U/[V], corresponding to the magnetic field, X data is time/[s].

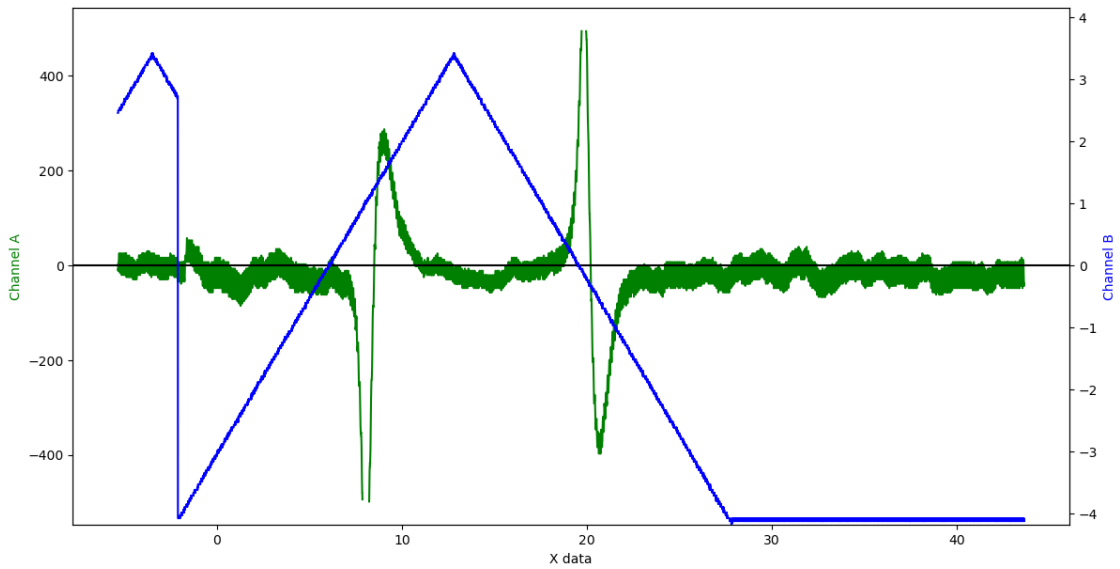

Figure 22: The output for the CuSO4 sample, $\theta = 100°$ .Chanel A is the voltage corresponding to the outgoing radiation/[mV], Chanel B is the voltage, U/[V], corresponding to the magnetic field, X data is time/[s].

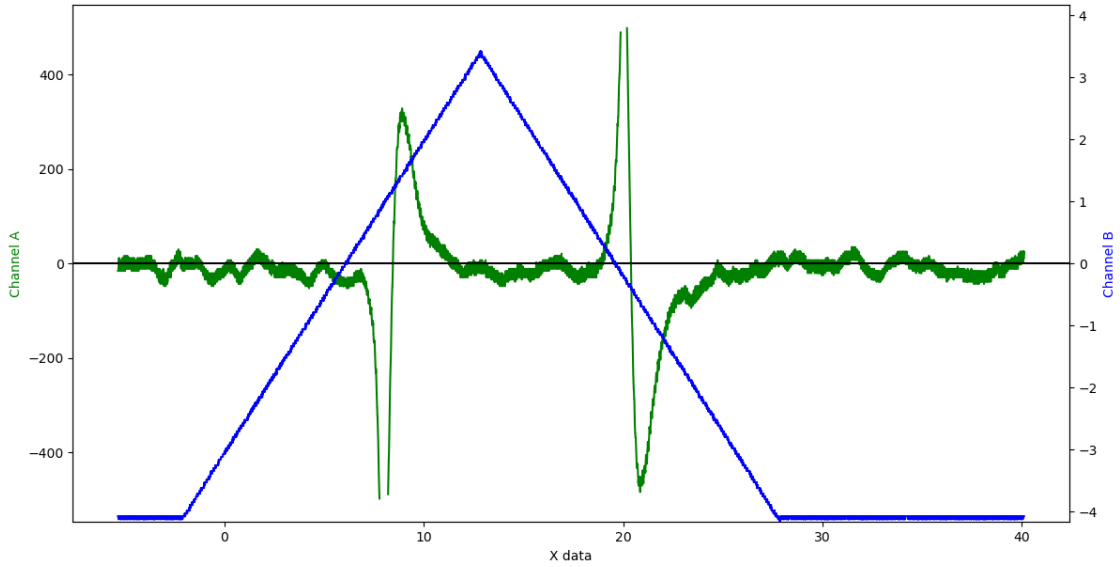

Figure 23: The output for the CuSO4 sample, $\theta = 110°$ .Chanel A is the voltage corresponding to the outgoing radiation/[mV], Chanel B is the voltage, U/[V], corresponding to the magnetic field, X data is time/[s].

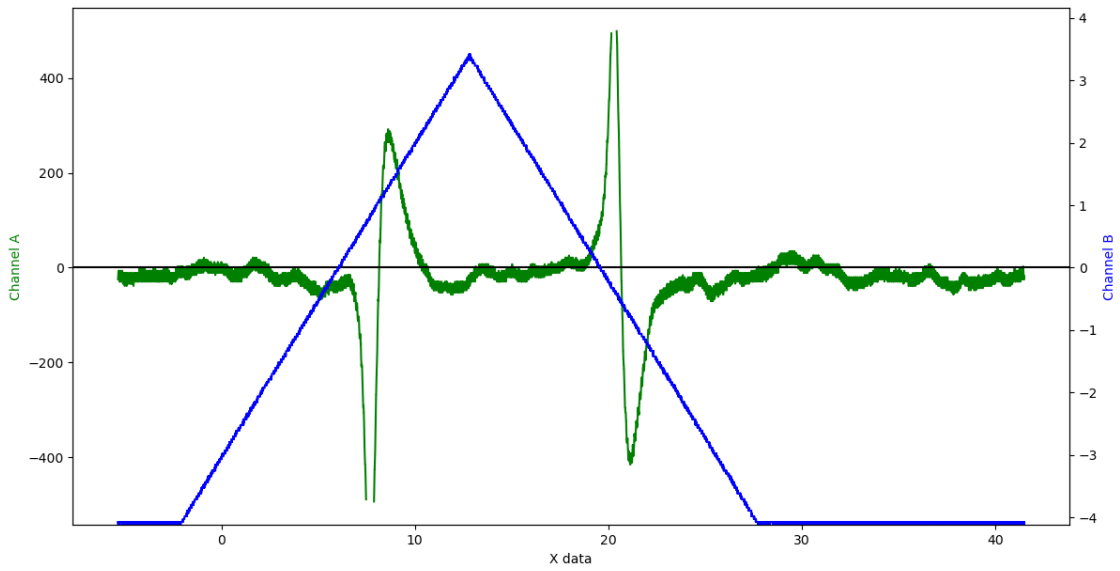

Figure 24: The output for the CuSO4 sample, $\theta = 120°$ .Chanel A is the voltage corresponding to the outgoing radiation/[mV], Chanel B is the voltage, U/[V], corresponding to the magnetic field, X data is time/[s].

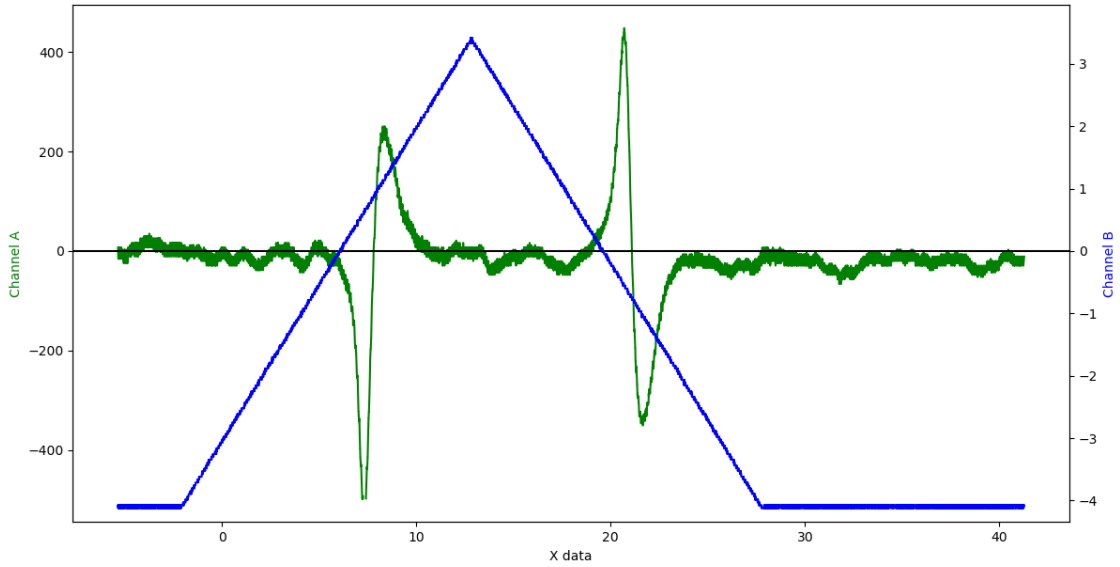

Figure 25: The output for the CuSO4 sample, $\theta = 130°$ .Chanel A is the voltage corresponding to the outgoing radiation/[mV], Chanel B is the voltage, U/[V], corresponding to the magnetic field, X data is time/[s].

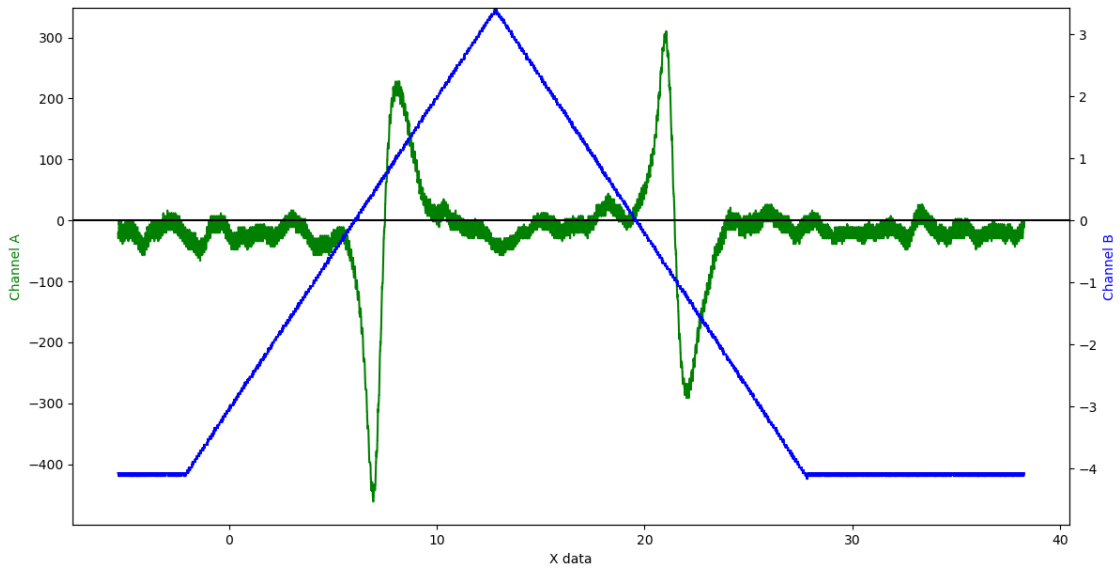

Figure 26: The output for the CuSO4 sample, $\theta = 140°$ .Chanel A is the voltage corresponding to the outgoing radiation/[mV], Chanel B is the voltage, U/[V], corresponding to the magnetic field, X data is time/[s].

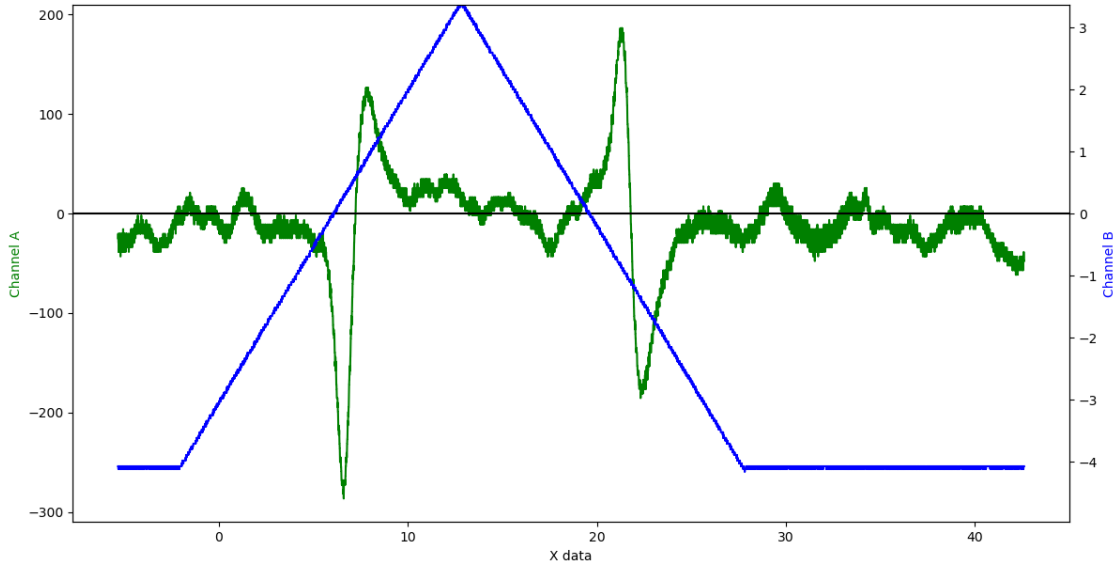

Figure 27: The output for the CuSO4 sample, $\theta = 150°$ .Chanel A is the voltage corresponding to the outgoing radiation/[mV], Chanel B is the voltage, U/[V], corresponding to the magnetic field, X data is time/[s].

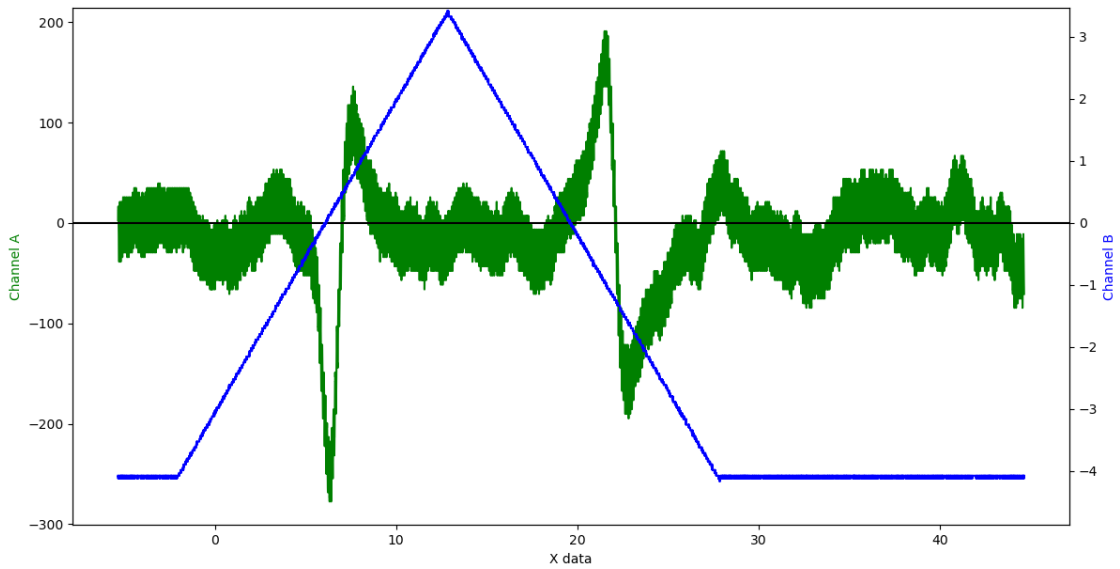

Figure 28: The output for the CuSO4 sample, $\theta = 160°$ .Chanel A is the voltage corresponding to the outgoing radiation/[mV], Chanel B is the voltage, U/[V], corresponding to the magnetic field, X data is time/[s].

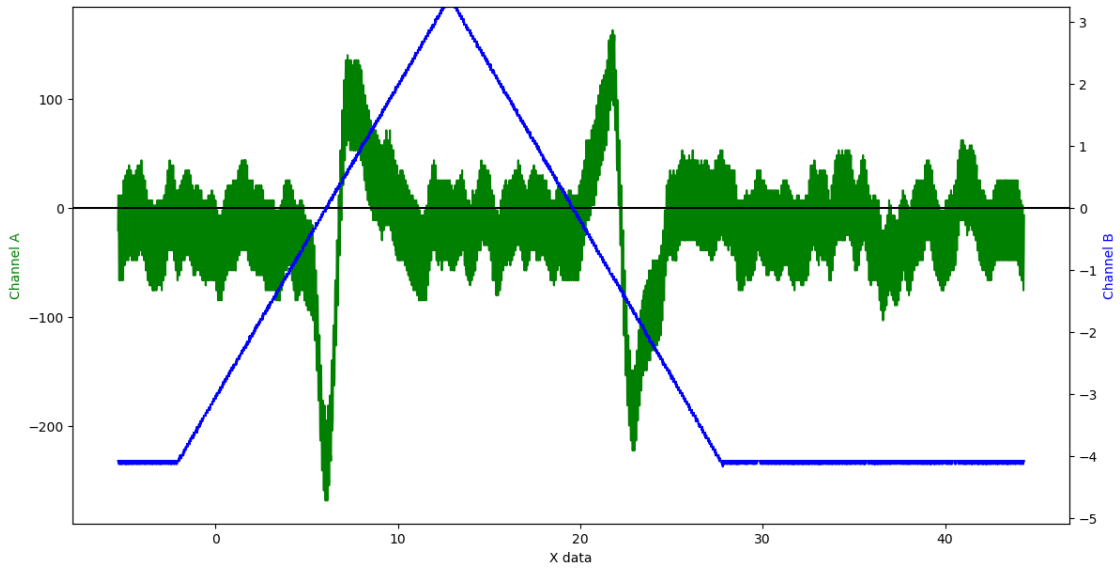

Figure 29: The output for the CuSO4 sample, $\theta = 170°$ .Chanel A is the voltage corresponding to the outgoing radiation/[mV], Chanel B is the voltage, U/[V], corresponding to the magnetic field, X data is time/[s].

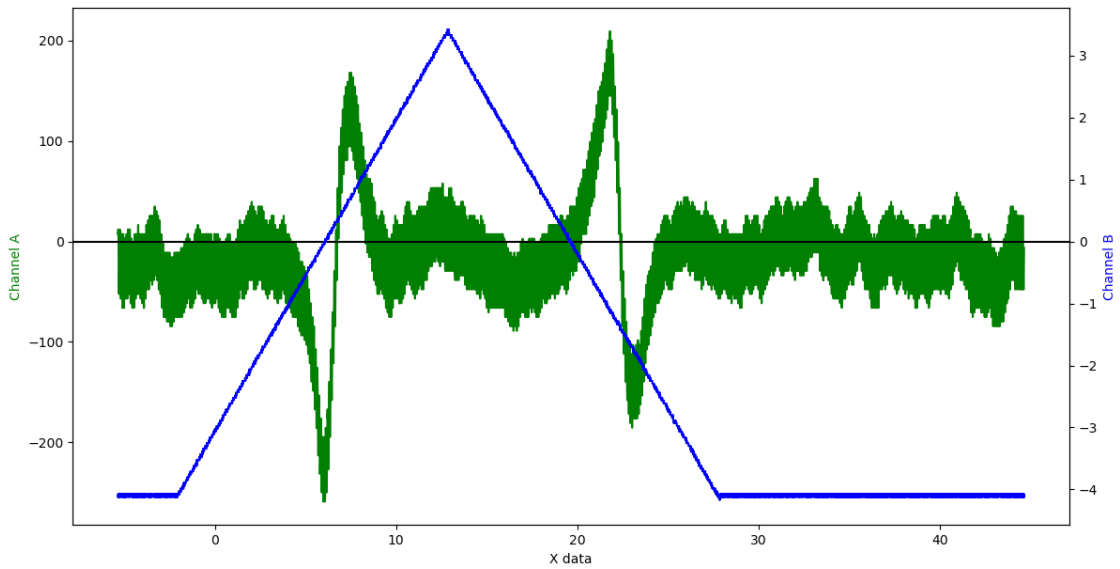

Figure 30: The output for the CuSO4 sample, $\theta = 180°$ .Chanel A is the voltage corresponding to the outgoing radiation/[mV], Chanel B is the voltage, U/[V], corresponding to the magnetic field, X data is time/[s].

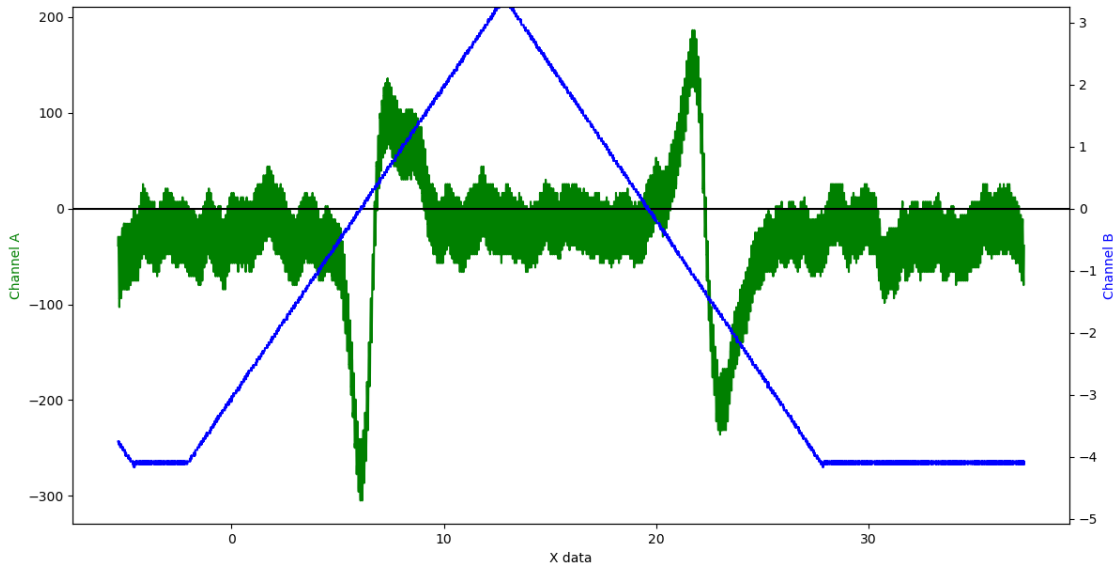

Figure 31: The output for the CuSO4 sample, $\theta = 190°$ .Chanel A is the voltage corresponding to the outgoing radiation/[mV], Chanel B is the voltage, U/[V], corresponding to the magnetic field, X data is time/[s].

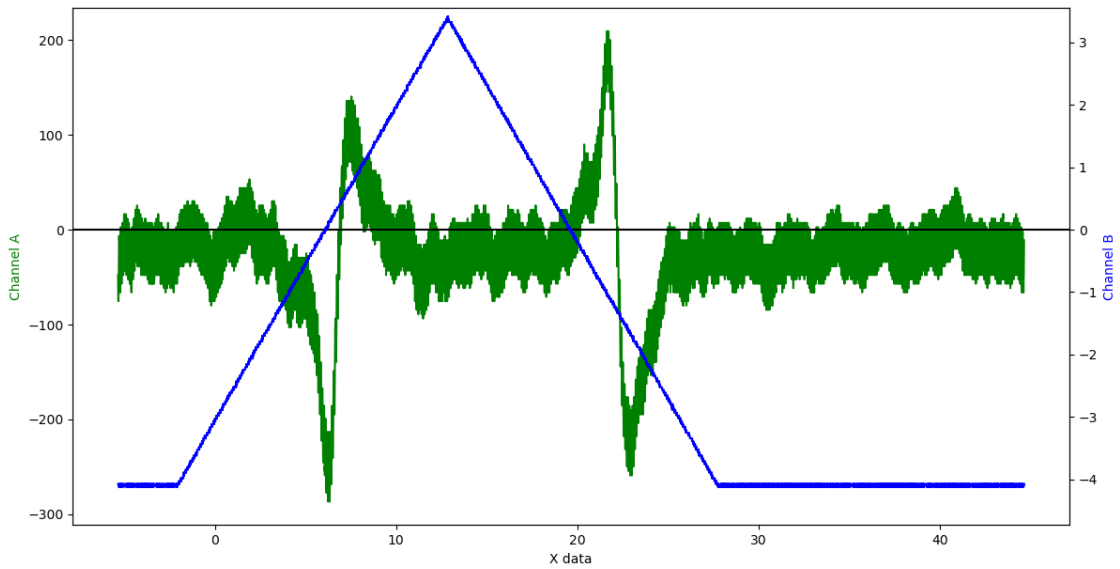

Figure 32: The output for the CuSO4 sample, $\theta = 200°$ .Chanel A is the voltage corresponding to the outgoing radiation/[mV], Chanel B is the voltage, U/[V], corresponding to the magnetic field, X data is time/[s].

References

[1] C. W. James, *Experimental notes for the ESR Practical*. StudOn, Advanced Laboratory Course, 2015.

[2] *TheoreticalBasics10*. StudOn, Advanced Laboratory Course.

[3] C.W. James, M. Tselengidou, *Preparation questions for FP-10: ESR*. StudOn, Advanced Laboratory Course.

[4] B. N. Figgis and R. Leckie, *The ISR g2 tensor in* CuSO4, 5H2O. Australian Journal of Chemistry 34, 2019-2023, 1981. URL: https://www.publish.csiro.au/ch/CH9812019

[5] *Physics 4E, Quantum Physics, Spring 2016, Zeeman Effect*. URL: https://courses.physics.ucsd.edu/2016/Spring/physics4e/zeeman.pdf

[6] Madhu, *What is the Difference Between Fine and Hyperfine Structure*, 2021. URL: https://www.differencebetween.com/what-is-the-difference-between-fine-and-hyperfine-structure

[7] *Magnetic Susceptibility*. Wikipedia. URL: https://en.wikipedia.org/wiki/Magnetic susceptibility

[8] Rolf Heid, *Electron-Phonon Coupling*, 2017. URL: https://www.cond-mat.de/events/correl17/manuscripts/heid.pdf